



HAL
open science

Control of self-assembly of amphiphilic wedge-shaped mesogens by combined magnetic field and temperature treatment

Denis V Anokhin, Ludmila L Gur'Eva, Kseniia N Grafaskaia, Evgeniy S Pikalov, Ainur F Abukaev, Viktor P Tarasov, Dimitri A Ivanov

► To cite this version:

Denis V Anokhin, Ludmila L Gur'Eva, Kseniia N Grafaskaia, Evgeniy S Pikalov, Ainur F Abukaev, et al.. Control of self-assembly of amphiphilic wedge-shaped mesogens by combined magnetic field and temperature treatment. *Physchem*, 2022, 2 (3), pp.274-285. 10.3390/physchem2030020 . hal-04291977

HAL Id: hal-04291977

<https://hal.science/hal-04291977v1>

Submitted on 17 Nov 2023

HAL is a multi-disciplinary open access archive for the deposit and dissemination of scientific research documents, whether they are published or not. The documents may come from teaching and research institutions in France or abroad, or from public or private research centers.

L'archive ouverte pluridisciplinaire **HAL**, est destinée au dépôt et à la diffusion de documents scientifiques de niveau recherche, publiés ou non, émanant des établissements d'enseignement et de recherche français ou étrangers, des laboratoires publics ou privés.

1 Article

2 Control of self-assembly of amphiphilic wedge-shaped 3 mesogens by combined magnetic field and temperature treat- 4 ment

5 Denis V. Anokhin ^{1,2,3,*}, Ludmila L. Gur'eva ², Kseniia N. Grafaskaia ^{2,4}, Evgeniy S. Pikalov ^{2,3}, Ainur F. Abukaev ^{2,5},
6 Viktor P. Tarasov ² and Dimitri A. Ivanov ^{1,2,3,6}

7 ¹ Sirius University of Science and Technology, 1 Olympic Ave, 354340, Sochi, Russia; deniano@yahoo.com
8 (D.V.A.),

9 ² Institute of Chemical Physics Problems of RAS, acad.Semenov av., 1, Chernogolovka, Russia;
10 gurieva@icp.ac.ru (L.L.G.), tarasov.07@list.ru (V.P.T.)

11 ³ Lomonosov Moscow State University, Leninskie Gory, 1, Moscow, Russia; pikasso99999@gmail.com (E.S.P.)

12 ⁴ Institute of Condensed Matter and Nanosciences, Université catholique de Louvain (UCLouvain), Croix du
13 Sud 1, box L7.04.02, Louvain-la-Neuve, 1348 Belgium; donnibrasko.92@mail.ru (K.N.G.)

14 ⁵ Moscow Institute of Physics and Technology (National Research University), Institutsky per. 9,
15 Dolgoprudny, Russia; abukaev.af@phystech.edu (A.F.A.)

16 ⁶ Institut de Sciences des Matériaux de Mulhouse-IS2M, CNRS UMR 7361, Jean Starcky, 15, F-68057 Mulhouse,
17 France; dimitri.ivanov@uha.fr (D.A.I)

18 * Correspondence: deniano@yahoo.com

19 **Abstract:** The report elucidates for the first time a significant effect of strong mag-
20 netic field combined with thermal treatment on the texture of thin liquid-crystalline films
21 in a smectic state. The metastable texture generated in magnetic field was arrested by
22 crystallization of mesogens during cooling to room temperature. The effect was demon-
23 strated on a series of wedge-shaped amphiphilic mesogens based on
24 1,2,3-tris-(dodecyloxy)benzene (TDOB): asymmetric 2,3,4-tris-(dodecyloxy)benzene sul-
25 fonic acid (TDOBSh) and its sodium (TDOBShNa) and pyridine (TDOBSPyr) salts. The
26 thermotropic properties and structure of liquid crystal phases of synthesized compounds
27 were addressed by differential scanning calorimetry, polarized optical microscopy and
X-ray diffraction. It was shown that depending on the type of counterion the synthesized
mesogens form different supramolecular structures. The largest effect of intense mag-
netic field was observed for the pyridine salt for which an ordered primitive cubic phase
texture was generated upon applying magnetic field normal with respect to the film. In
contrast, for the corresponding acid an improvement of gyroid cubic phase orientation
was detected under magnetic field oriented along the film. A highly ordered columnar
phase of the sodium salt showed a minimal effect of magnetic field.

28 **Citation:** Lastname, F.; Lastname, F.;
29 Lastname, F. Title. *Physchem* **2022**, *2*,
30 Firstpage–Lastpage.
31 <https://doi.org/10.3390/xxxxx>

32 Academic Editor: Firstname
33 Lastname

34 Received: date

Accepted: date 35

Published: date

36 **Publisher's Note:** MDPI stays
37 neutral with regard to jurisdictional
38 claims in published maps and
institutional affiliations.



39 **Copyright:** © 2022 by the author
40 Submitted for possible open access
41 publication under the terms and
42 conditions of the Creative Commons
43 Attribution (CC BY) license
44 (<https://creativecommons.org/licenses/by/4.0/>).
45

Keywords: wedge-shaped amphiphilic mesogens; 2,3,4-tris-(dodecyloxy)benzene sulfonates;
orientation in magnetic field; differential scanning calorimetry; grazing-incidence X-ray diffraction

1. Introduction

One of the most powerful tools employed for development of smart, sensitive ma-
terials is the molecular self-assembly [1]. The unique properties of supramolecular
structures include the ability of spontaneous formation and easy transformation under
the influence of external factors (temperature, pressure, chemical environment, irradi-
ation, magnetic and electric fields, etc.) due to the dynamic nature of weak intermolecular
bonds, such as electrostatic, van der Waals or hydrogen interactions. The structure of

46 such molecular "building blocks" is determined both by the shape and size of the original
47 molecules and the position of functional groups [2]. External factors shift the balance of
48 these interactions stimulating a change in molecular conformation and, consequently,
49 phase transition to a new structure. In particular, application of magnetic field could in
50 some instances generate a texture which would be not thermodynamically stable and
51 therefore not easily achievable in the absence of the field such as the so-called
52 homeotropic orientation discussed later.

53 Wedge-shaped amphiphilic mesogens based on tris(alkyloxy)benzene sulphonic
54 acid is a relatively new class of self-assembling molecules [3, 4]. They can serve as
55 building blocks for synthesis of novel functional materials, such as highly regular poly-
56 meric ion-conductive membranes, nanoreactors and drug delivery systems. Variation of
57 chemical composition (change in alkyl chain length, substitution of counterion, addition
58 of azobenzene group) or external factors (temperature change, presence of saturated
59 solvent vapor atmosphere with different polarity, UV-irradiation) allow to form crystal-
60 line or liquid-crystalline phases of different symmetry.

61 Self-assembly of amphiphilic mesogens seems as a promising "bottom-up" ap-
62 proach for fabrication of membranes with highly-defined size and topology of ion
63 channels which can become alternative to Nafion or zeolites as efficient pro-
64 ton-conductive membrane for application of perspective fuel cells. [5-7]. The proton
65 transport across the membranes built from such molecules can be optimized using ex-
66 ternal stimuli during film preparation [8]. The most common mesophase structures for
67 thin films of mesogens containing ion channels are columnar (hexagonal and monoclinic)
68 and smectic. Such liquid-crystalline films demonstrate textures having mainly in-plane
69 orientation of the channels which is not optimal for proton transport across the mem-
70 brane. To achieve optimal membrane efficiency, it is necessary to increase the number of
71 channels for proton transport across the membrane, which is possible when the channels
72 are normally, or homeotropically, oriented with respect to the membrane film surface.
73 However, switching the channels' orientation to normal or homeotropic is limited by
74 thermodynamic instability of such a texture [9-11]. One of the ways to provide stable
75 homeotropic texture in thin films is to apply a magnetic field to the mesogens in isotropic
76 or LC state and then fix it by chemical bonding [12-15]. The membranes based on
77 polymerizable wedge-shaped amphiphilic LCs were shown to form highly ordered
78 mesophases in magnetic field resulting an increase of their conductivity by two orders of
79 magnitude as compared to unoriented materials [15]. It is important to mention that re-
80 orientation of mesogens in magnetic field mainly occurs in nematic LC state which is
81 characterized by low degree of molecular ordering. For columnar phases, magnetic field
82 was found to only enhance the thermodynamically stable planar orientation [15].

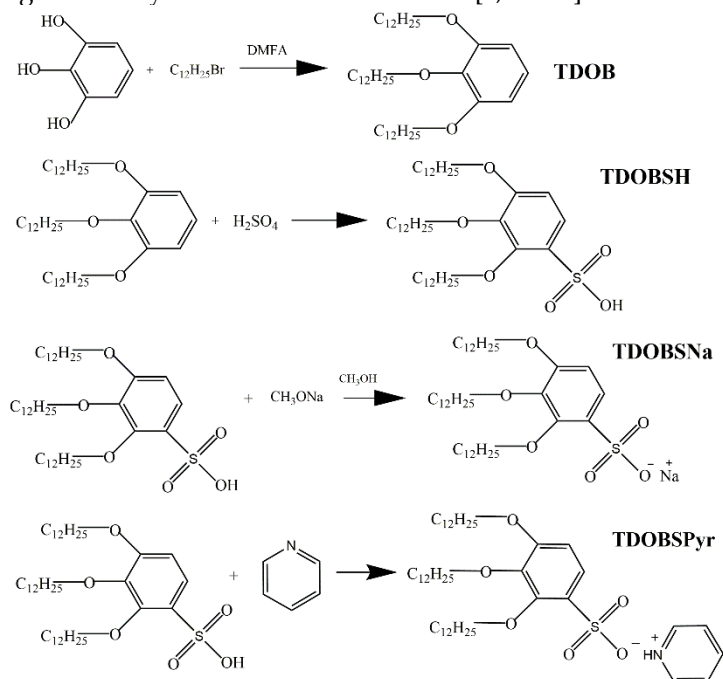
83 Derivatives of symmetric [4, 16-18] and asymmetric [3, 19-22] tris(alkyloxy)benzene
84 sulfonic acid exhibit a variety of both crystalline and thermotropic liquid-crystalline
85 mesophases, including smectic, cubic, ordered and disordered columnar mesophases
86 [19-22]. These phases can be stabilized by physical and chemical cross-linking to form
87 polymer membranes with well-controlled ion channel topologies [4, 8].

88 Summarizing, the development of approaches to control the orientation of
89 ion-conducting channels in self-organized systems of wedge-shaped amphiphilic LC
90 compounds is of great interest [3, 4, 8, 16-22]. In the present work, a combined effect of
91 high-temperature annealing and magnetic field was addressed for wedge-shaped
92 amphiphilic mesogens: asymmetric 2,3,4-tris-(dodecyloxy)benzene sulfonic acid
93 (TDBOSH) as well as its sodium (TDBOSNa) and pyridine (TDBOSPyr) salts. These
94 compounds demonstrate complex thermotropic behavior with formation of both crystal-
95 line and liquid crystalline phases. This opens perspectives for design of thin films with
96 unusual texture by application of strong external stimulus like magnetic field on the films
97 in LC state with high molecular mobility with following fixing of desired supramolecular
98 morphology by crystallization at room temperature.

2. Materials and Methods

2.1. Synthesis

The TDBOSH, TDBOSNa and TDBOSPyr were synthesized according to the following scheme by the methods described in [4, 19-22]:



Scheme 1. Synthesis of TDOB, TDBOSH, TDBOSNa and TDBOSPyr.

2.2. Reagents

Pyrogallol (99%), 1-bromododecane (95%), pyridine (99.8%), sodium methylate (pure, anhydrous) (Sigma-Aldrich), benzene (Cd, Ecos), acetone, sulphuric acid, potassium carbonate (CH, Chemmed) were used without further purification. Molecular sieves 4A (granules, diameter 3.2 mm, Acros Organics) were calcinated under vacuum at 250 oC. Dimethylformamide (DMFA) (99.8%, Sigma-Aldrich) was dehydrated by azeotropic distillation with benzene at atmospheric pressure, incubated over molecular sieves 4A for 3 days, followed by vacuum distillation under argon current. The methanol (Cr, Chemmed) for recrystallization was distilled over molecular sieves 4A.

2.3. Methods of the analysis

Identification of the synthesized compounds was carried out by IR, ^1H NMR and ^{13}C NMR spectroscopy and elemental analysis. IR spectra were taken in KBr tablets using Specord M80 spectrometer with Soft Spectra software. Two-dimensional Cosy and HSQC NMR spectra were measured in CDCl_3 solution with trimethylsilane (TMS) reporter on AVANCE-III-500 spectrometer and were interpreted using Mest ReNova 12-0-0 Manual software. Elemental analysis was performed on Vario EL cube equipment (Elementar GmbH).

Thermotropic properties of compounds were determined by the differential scanning calorimetry (DSC) methods using "DSC 30 Mettler Toledo Star System" in the temperature range from -40 to 140°C with scanning rate of 5 deg/min . In order to check the reversibility of phase transitions two DSC heating-cooling ramps were performed for all samples.

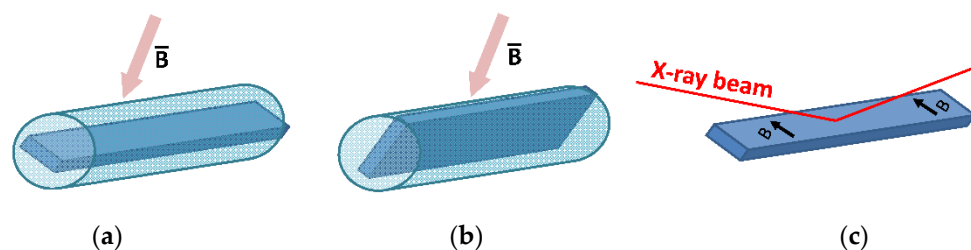
Thin films (200-500 nm) for POM and GIXD experiments were prepared by spin-coating of 10 mg/ml solution in chloroform on a silicon substrate at a rate of 1000 rpm . For NMR experiments the samples were prepared by drop-casting of 20 mg/ml so-

130 lution in chloroform on a silicon substrate. Then the drop-casted films were annealed at
131 85°C for 1 hour in vacuum oven.

132 The effect of thermal history on texture of the thin films of the synthesized com-
133 pounds was studied by polarized optical microscopy (POM). The spin-coated films were
134 annealed in normal atmosphere at 85°C for 3 hours using Linkam LTS420 thermal stage.
135 Optical measurements of the as-cast and annealed films were carried out with a Karl
136 Zeiss Axio Scope A1Pol microscope in polarized light.

137 The structure of unoriented samples was studied by X-ray diffraction (XRD) on
138 custom-built WAXS/SAXS X-ray System diffractometer with a 1.54 Å wavelength
139 equipped with a two-dimensional Pilatus 300k detector. The sample-detector distance
140 was 1.15 m. The modulus of the scattering vector \mathbf{s} ($|\mathbf{s}| = 2\sin\theta/\lambda$, where θ is the Bragg
141 angle, λ is the wavelength and $|\mathbf{s}|$ is the norm of the \mathbf{s} vector) was calibrated using sev-
142 eral diffraction orders of silver behenate. To exclude the influence of humidity the
143 measurements were carried out in vacuum. Analysis of X-ray data, including back-
144 ground subtraction and radial integration of 2D diffractograms was performed with
145 procedures developed in the IgorPro (Wavemetrics Ltd.) environment.

146 To address the effect of magnetic field (MF) on thin film texture, the capillary with
147 sample on substrate was placed into resonator of BRUKER-500 NMR spectrometer (pro-
148 ton frequency 400 MHz). Magnetic induction 9.5 Tesla was oriented normal to the capil-
149 lary axis. As it was shown in [15] such intensity is sufficient for reorganization of ben-
150 zene-containing molecules in LC phase. Orientation of \mathbf{B} vector of MF to set it normal
151 (Fig. 1a) or parallel (Fig. 1b) to the film surface was achieved by rotation of the capillary
152 around its axis. Then, the samples were heated to temperatures above isotropization
153 point (85°C for TDBOSH and TDBOSPy, 110°C for TDBOSNa) and slowly cooled down
154 to room temperature. During cooling NMR spectra of the films were recorded.
155



156
157 **Figure 1.** Schematic of the sample orientation in the capillary normal (a) and parallel
158 (b) to the MF (pink arrow); (c) Orientation of X-ray beam in respect to MF direction
159 during GIXD measurements.

160 The texture of the films after MF exposure was addressed by grazing-incidence
161 X-ray diffraction (GIXD) at the BM26 beamline of the European Synchrotron Radiation
162 Facility (Grenoble, France). The measurements were performed at a wavelength of 1.03 Å
163 and the diffraction signal was recorded with a 2D Pilatus 300k detector. The indexation of
164 2D diffractograms was made in procedures built in IgorPro (Wavemetrics Ltd.) software.
165 For films oriented parallel to the MF, X-ray beam was oriented normally to the direction
166 of MF (Fig. 1c).

167 3. Results

168
169 The DSC thermograms of the synthesized mesogens TDOBSH, TDOBSNa and
170 TDOBSPyr are presented in Fig. 2, and their thermal parameters are summarized in Table
171 1.

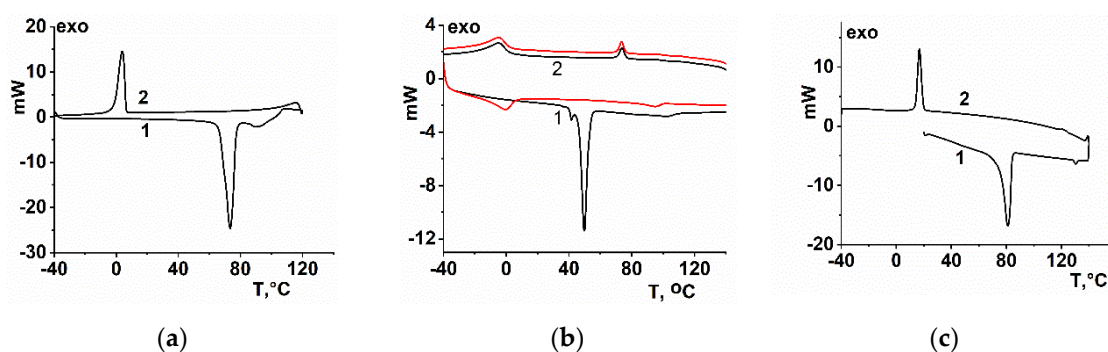


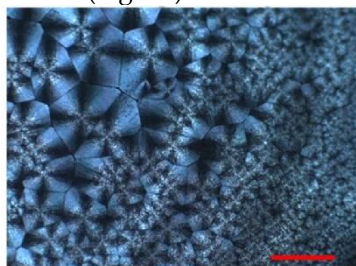
Figure 2. DSC heating (1) and cooling (2) thermograms for mesogens: (a) TDOBSH, (b) TDOBSNa (1st cycle – black line, 2nd cycle – red line), (c) TDOBSPy. Exo peaks are positive. Scanning rate 5°C/min.

The precursor TDOB has a single endothermic melting peak of isotropization of crystalline phase (Table 1), which indicates the absence of LC state. The second endothermic peak both on first and on second DSC heating ramps in the region 90-130°C shows isotropization of LC phase (see Figure 2 and Table 1). The found values transition temperatures are close to the literature data [3, 4, 16 - 22].

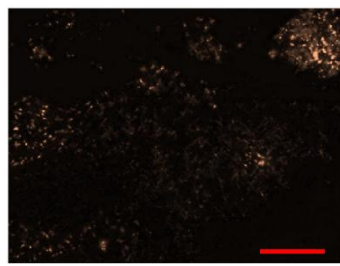
Table 1. Thermal parameters of TDOB, TDOBSH, TDOBSNa and TDOBSPy measured by DSC

Sample	Heating				Cooling	
	T ₁ , °C	ΔH, J/g	T ₂ , °C	ΔH, J/g	T ₁ , °C	T ₂ , °C
TDOB	42.9	188.8	-	-	21.5	-
TDOBSH						
1 st heating	72.7	99.0	90.0	5.1	-	4.1
2 nd heating	6.8	-	17.0	-	10.8	-0.7
TDOBSNa						
1 st heating	49.7	46.7	105.0	4.2	73.7	-4.8
2 nd heating	-0.7	-	94.0	-	73.6	-4.6
TDOBSPy						
1 st heating	79.7	105.9	128.3	1.7	120.0	17.9

To improve the texture of thin films of the studied sulphonates the samples were annealed in the temperature window of existence of LC phase between T₁ and T₂. From one hand, at this temperature the molecular mobility is enhanced to reach thermodynamically equilibrium phase and large ordered domains. From another hand, the thin films in LC state keep a certain mechanical stability, whereas isotropization can lead to dewetting and other negative factors. As-cast and annealed films were studied by POM. The formation of spherulitic textures typical for crystalline material is observed for TDOBSH as-cast film (Fig. 3a). After annealing of the films, the birefringence largely disappears indicating either isotropization or formation of optically inactive cubic phase (Fig. 3b).



(a)



(b)

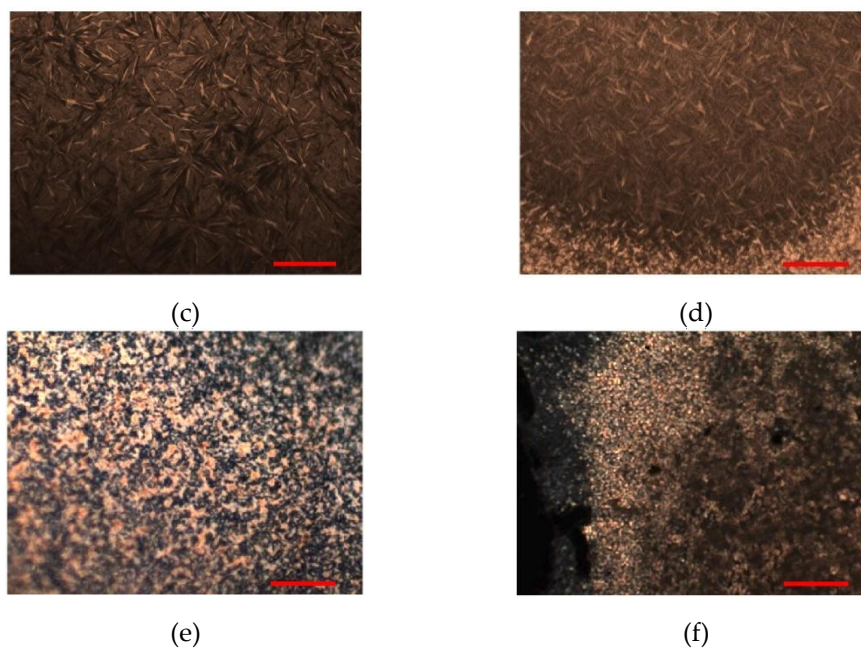
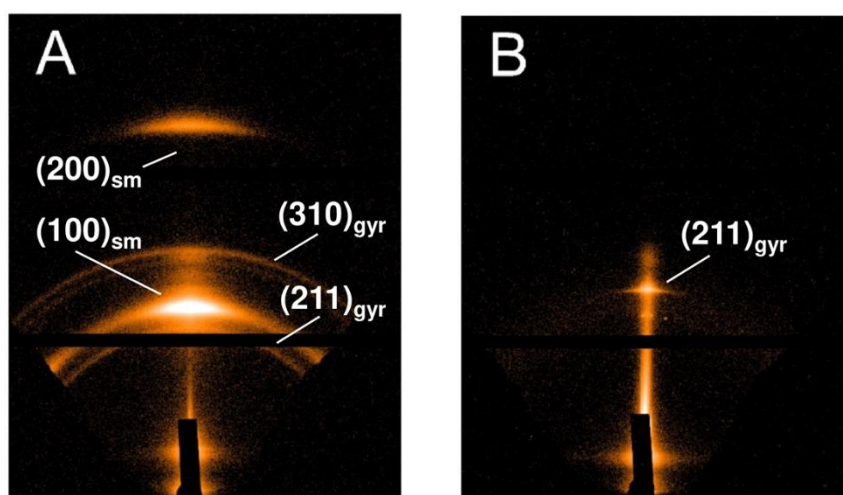


Figure 3. Optical micrographs of films before and after annealing for: TDOBSH (a, b); TDOBSNa (c, d); TDOBSPyr (e, f). The scalebar is 50 mkm.

The POM image of as-cast film of sodium salt shows optically active needle-like domains typical for smectic or columnar LC phase (Fig. 3c). Annealing at 85°C results in growth of optical activity and appearing of granular texture (Fig. 3d). Presence of bulky pyridinium counterion significantly changes self-assembly of thin film. Microphotographs of the as-cast film of TDOBSPyr show a fine-grained structure with low optical activity (Fig. 3e). Annealing leads to a decrease in optical density indicating the formation of a cubic phase (Fig. 3f). Thus, depending on the type of counterion and thermal pre-history the synthesized mesogens reveal a variety of supramolecular structures.



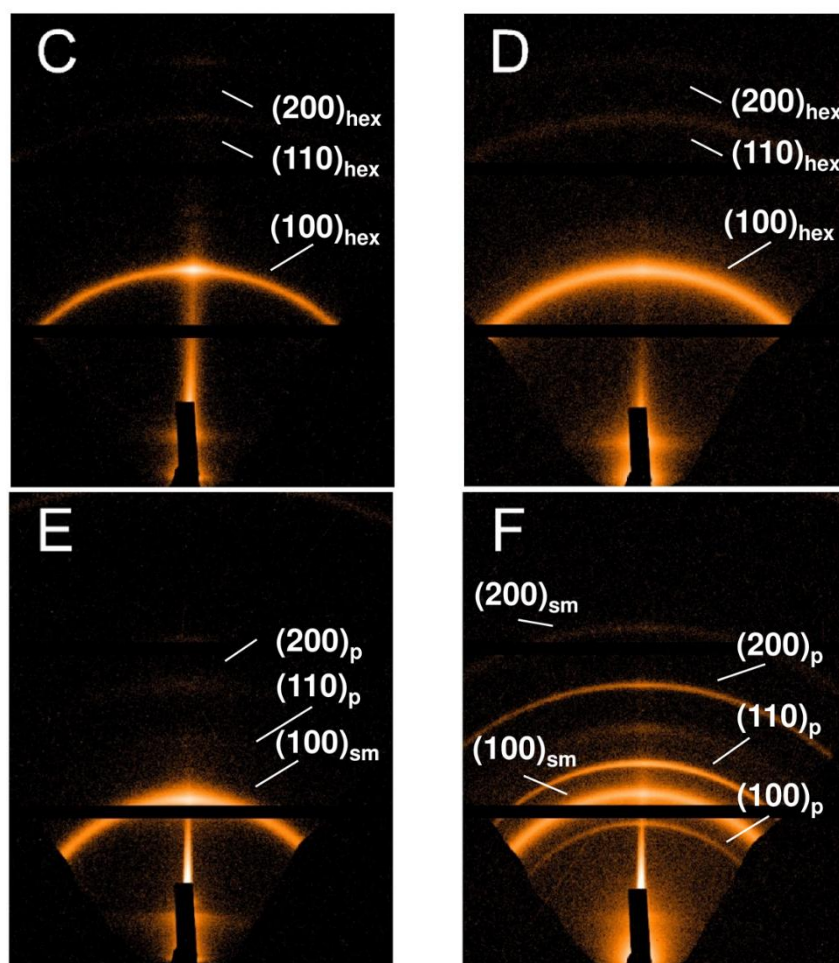


Figure 4. 2D GIXD patterns of TDOBSH (a,b), TDOBSNa (c,d) and TDOBSPyr (e,f) before (a,c,e) and after (b,d,f) annealing. The most intense reflections are marked with white arrows and indexed according to smectic (sm), gyroid (gyr), columnar hexagonal (hex) and cubic primitive (p) phases. The film was oriented horizontally. The black regions appear after background subtraction.

A detailed analysis of the crystalline and LC structure of the thin films was made by GIXD technique. Investigation of the as-cast thin films of TDOBSH shows formation of smectic structure with lattice parameter $a_{sm}=36.8 \text{ \AA}$ and a small fraction of gyroid cubic phase with parameter $a_{gyr}=98.0 \text{ \AA}$ (Fig. 4a) [23]. During annealing of the sample at 85°C the smectic phase transforms into thermodynamically stable gyroid structure with decreased parameter $a_{gyr}=98.0 \text{ \AA}$ (Fig. 4b). The GIXD patterns of TDOBSNa indicate presence of hexagonal columnar phase with $a_{hex} = 36.6 \text{ \AA}$ in both as-cast and annealed films (Fig. 4c,d). The increase of half-width of the reflections after annealing indicates a certain growth of grain-like domains without any preferential orientation. The analysis of GIXD diffractograms of as-cast films of TDOBSPyr reveals the self-assembly similar to TDOBSH (Fig. 4e,f). During annealing the smectic phase ($a_{sm}=41.3 \text{ \AA}$) transforms to Im3hm cubic phase with $a_p = 48.4 \text{ \AA}$. Formation of primitive cubic phase was detected earlier for wedge-shaped sulfonates with potassium cation at high temperature [21]. Consequently, formation of Im3hm cubic phase in thin film of TDOBSPyr can be explained by the presence of bulky pyridinium counterion. The results of indexation are summarized in Table 2.

Table 2. Indexation of GIXD patterns of thin films

Sample	As-cast films			After annealing			
	Phase	hkl	d_{exp} , Å	Phase	hkl	d_{exp} , Å	
TDOBSH	Sm $a_{\text{sm}} = 36.9$ Å	100	36.9	Cub _{gyr} $a_{\text{gyr}} = 93.2$ Å	211	37.9	
		200	18.6		220	33.3	
		211	41.4		310	29.3	
	Cub _{gyr} $a_{\text{gyr}} = 98.0$ Å	310	29.9				
		222	28.2				
TDOBSPyr	Sm $a_{\text{sm}} = 41.3$ Å	100	41.3	Sm $a_{\text{sm}} = 40.0$ Å	100	40.0	
		200	20.7		200	20.0	
		300	13.9		300	13.3	
	Cub _p $a_{\text{p}} = 48.4$ Å	200	24.2		100	48.4	
					Cub _p	110	33.9
					$a_{\text{p}} = 48.5$ Å	111	29.0
						200	24.2
TDOBSNa	Col _h $a_{\text{hex}} = 36.6$ Å	100	31.7	Col _h $a_{\text{hex}} = 36.2$ Å	100	31.5	
		110	18.4		110	18.3	
		200	15.9		200	15.6	

One can see that variation of the type of counterion allows changing thermal and phase behavior of the synthesized mesogens, as well as the topology of ion channels. The existence of liquid-crystalline state at elevated temperature can be explained by disordering of linear alkyl chains and increase of local molecular mobility [8]. However, for practical application of synthesized compounds as proton-conductive membrane it is important to provide homeotropic orientation of water channels in columnar and smectic phase. After formation of such thermodynamically metastable state at elevated temperature, it can be consequently fixed by crystallization of the mesogens during cooling to room temperature without disturbance of supramolecular organization. The effective external stimulus for formation of metastable homeotropic LC texture is application of strong magnetic field assessable in NMR spectrometer.

Fig. 5 shows NMR spectra of synthesized mesogens in LC state obtained at different temperatures on a BRUKER 500 spectrometer with a proton frequency of 500 MHz. The narrow line at ~1 ppm on NMR spectra of TDOBSH corresponds to acid protons (Fig. 5a). Similar peak is visible for TDOBSNa indicating formation of a crystalline hydrate with one water molecule (Fig. 5b). The variation of structure was detected only after cooling to 24°C. The narrow peak in Fig. 5c corresponds to the hydrogen bonding of the mesogen and pyridinium proton of TDOBSHPyr. As expected, intensity of this line increases during heating indicating the self-assembly of the material.

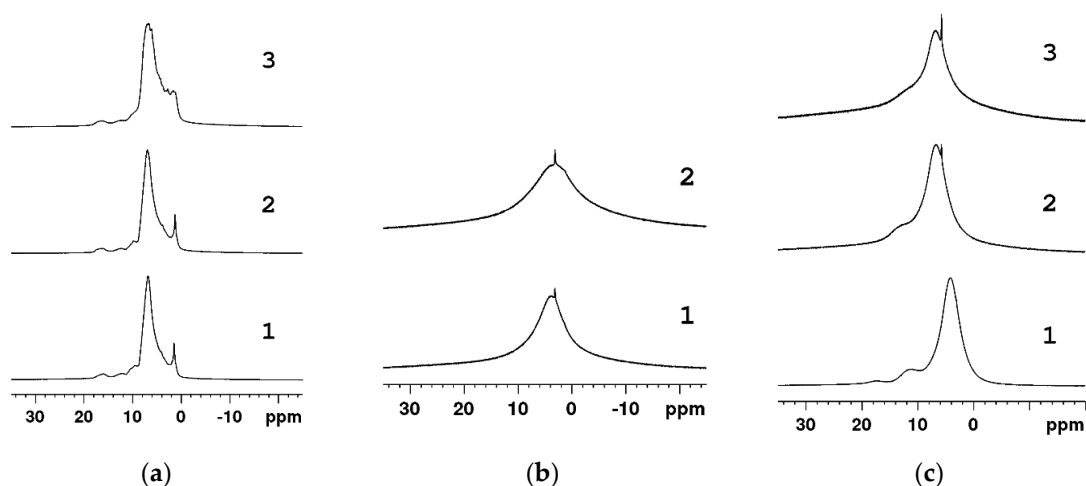


Figure 5. NMR spectra of synthesized mesogens: (a)- TDOBSH at 80°C (1), 50°C (2) and 30°C (3); (b) - TDOBSNa at 80°C (1), 24°C (2); (c) - TDOBSPyr at 80°C (1), 50°C (2), 30°C (3).

The effect of magnetic on thin films texture was studied by GIXD using synchrotron source. Fig. 6a-c shows 2D GIXD diffractograms for TDOBSH thin film before and after MF. Application of MF parallel to the film surface results in orientation of initially isotropic gyroid cubic phase and appearance of a small fraction of smectic phase (Fig. 6b). For the gyroid lattice the 211 vector is oriented normal to the substrate. For normal orientation of MF the GIXD pattern demonstrates two weak meridional reflections of the gyroid phase (Fig. 6c). Consequently, parallel alignment of MF stimulates development of large well-oriented domains of the cubic phase. For sodium salt we do not observe significant changes in hexagonal phase texture after application of MF parallel to the film compare to non-exposed annealed sample (Fig. 6d,e). However, normal orientation of MF causes a certain disorientation of the hexagonal phase and appearance of a weak peak in small-angle region which can be attributed to less stable smectic phase (Fig. 6f). Thus, normal orientation of MF prevents formation of large regular domains of the columnar hexagonal mesophase. For pyridinium salt self-assembly of mesogens in MF parallel to the film leads to a partial transformation of initial oriented primitive cubic phase to smectic phase (Fig. 6g,h). In contrast, MF oriented normal to the film stimulates formation of mixture of unoriented and well-oriented primitive Im3hm cubic phase with 100 vector oriented normal to the surface (Fig. 6i). The difference in the effect of MF orientation on the texture improvement for TDOBSPyr can be explained by interaction of MF with pyridinium rings.

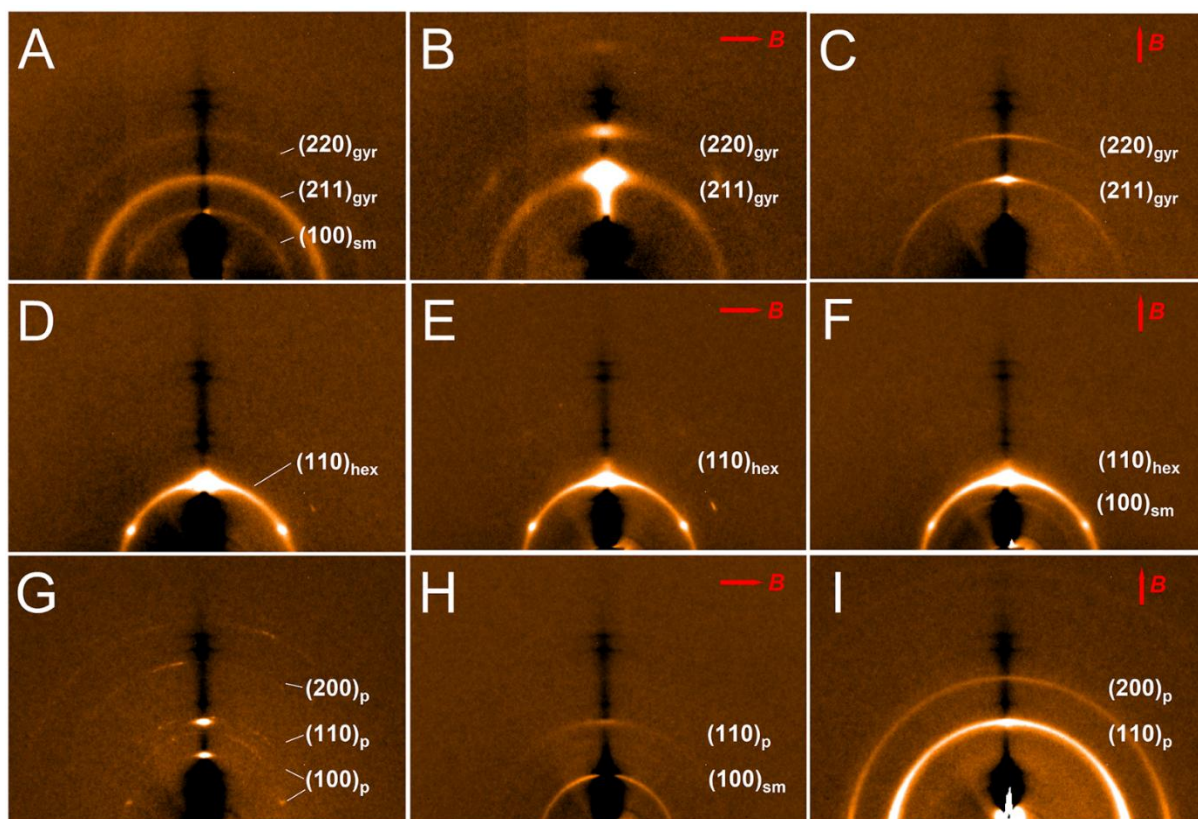


Figure 6. 2D GIXD patterns of TDOBSH (a-c), TDOBSNa (d-f) and TDOBSPyr (g-i): left column – before application of MF, middle column – with MF parallel to the film, right column – with MF normal to the film. The most intense reflections are marked with white arrows and indexed according to smectic (sm), gyroid (gyr), columnar hexagonal (hex) and cubic primitive (p) phases. The film was oriented horizontally. Red arrow indicates direction of magnetic field in respect to the film surface. The black regions appear after background subtraction.

The presented diffractograms confirm the effectiveness of the magnetic field on the texture and degree of ordering of amphiphilic mesogens. The largest effect of the magnetic field is observed for the pyridine salt, which is probably explained by a weak ordering of the mesogen molecules in the initial film and magnetic susceptibility of the pyridinium. A fraction of highly ordered primitive cubic phase is formed as a result of MF exposure. For the acid, on the other hand, a decrease in the initial cubic phase is observed, possibly due to rapid cooling of the sample in the NMR instrument. For the highly ordered columnar phase of the sodium salt the effect of MF application in both directions is minimal.

4. Conclusions

In this work, reorganization of texture of thin liquid-crystalline films in a smectic state was shown for the first time. It is noteworthy that the field-induced texture is metastable without magnetic field (MF) but can be fixed due to ability of the compounds to crystallize at room temperature and thereby create a physical network of crystalline domains. To this end, we synthesized derivatives of a wedge-shaped amphiphilic mesogen - asymmetric 2,3,4-tris(dodecyloxy)benzene sulfonate and its pyridine and sodium salts. The processes of self-assembly of synthesized mesogens in bulk and in thin films were preliminarily addressed by DSC, POM and GIXD. The influence of MF oriented along or normal to the film surface on the supramolecular structure formation at different temperatures was studied. It was found that depending on the counterion nature the samples demonstrate specific thermotropic behavior and form different

297 supramolecular structures. For thin films of TDOBSH high-temperature annealing results
298 in transition from a metastable smectic LC phase to a cubic bicontinuous gyroid phase.
299 Applying of MF parallel to the film surface stimulates alignment of the cubic domains. In
300 contrast, orientation of MF normal to the substrate hinders growth of regular domains of
301 gyroid phase during slow cooling from the LC state to room temperature. The sodium
302 salt (TDOBSNa) demonstrates formation of columnar hexagonal LC phase irrespective of
303 the thermal history. We speculate that application of MF along the normal direction
304 slightly disturbs the growth of large columnar domains due to appearance of metastable
305 smectic phase.

306 Among all the studied molecules the most pronounced effect of MF on self-assembly
307 was detected for the pyridinium salt. The stable Im3hm cubic phase forming during an-
308 nealing completely disappears under the action of MF oriented along the TDOBS_{Pyr} film.
309 Realignment of the mesogens results in appearance of the smectic phase typical of the
310 as-cast films. In contrast, the normally oriented MF improves the development of large
311 highly-oriented domains of Im3hm cubic phase during cooling. The reason of specific
312 behavior of TDOBS_{Pyr} in MF could be due to anisotropy of magnetic susceptibility of
313 pyridine. The obtained results can help for development of strategy for fabrication of
314 novel proton-conductive membranes built by “bottom-up” approach.
315

316 **Author Contributions:** Conceptualization, D.V.A.; Data curation, A.F.A.; Formal analysis, K.N.G.;
317 Investigation, E.S.P.; Methodology, V.P.T.; Supervision, D.V.A.; writing — original draft prepara-
318 tion, L.L.G.; Writing — review and editing, D.A.I. All authors have read and agreed to the pub-
319 lished version of the manuscript.

320 **Funding:** The synthetic part of the work was funded by State orders No. 0089-2019-0012 (state
321 registration number AAA-A19-119032690060-9) and No. 0089-2019-0002 (state registration number
322 AAA-A19-119071190017-7). The structural characterization of the phases and orientation was
323 funded by the Sirius University of Science and Technology.

324 **Data Availability Statement:** The data presented in this study are available in article

325 **Acknowledgments:** The authors thank the IPCP RAS Analytical Center for the 1H and 13C NMR
326 tests and for the elemental analysis and M. Rosenthal (BM26, ESRF) for GIXD experiments.

327 **Conflicts of Interest:** The authors declare no conflict of interest.

328 References

- 329 1. Antipin, I.S.; Alémov, M.V.; Arslanov, V.V.; Burilov, V.A.; Vatsadze, S.Z. et al. Functional supramolecular systems: design and
330 applications. *Russ. Chem. Rev.* **2021**, *90*(8), pp. 895-1107.
- 331 2. Alfutimie, A.; Curtis, R.; Tiddy, G.J.T. Lyotropic Surfactant Liquid Crystals: Micellar Systems. *In Handbook of Liquid Crystals*,
332 2nd ed.; Goodby, J., Collings, P., Kato, T., Tschierske, C., Gleeson, H., Raynes, P., Vill, V., Eds. Wiley-VCH: Weinheim, Ger-
333 many, 2014; Volume 6.
- 334 3. Li, L.; Rosenthal, M.; Zhang, H.; Hernandez, J.; Drechsler, M.; Phan, K.H.; Rütten, S.; Zhu, X.; Ivanov, D.A.; Möller, M.
335 Light-Switchable Vesicles from Liquid-Crystalline Homopolymer-Surfactant Complexes. *Angew. Chem. Int.* **2012**, *51*,
336 11616-11619.
- 337 4. Zhang, H.; Li, L.; Möller, M.; Zhu, X.; Hernandez, J.; Rueda, J.; Rosenthal, M.; Ivanov, D. A. From Channel-Forming Ionic
338 Liquid Crystals Exhibiting Humidity-Induced Phase Transitions to Nanostructured Ion-Conducting Polymer Membranes.
339 *Adv. Mater.* **2013**, *25*, 3543-3548.
- 340 5. Mauritz, K. A.; Moore, R.B. State of Understanding of Nafion. *Chem. Rev.* **2004**, *104*(10), 4535-4586.
- 341 6. Allison, S.A.; Barrer, R.M. Sorption in the β -phases of transition metal(II) tetra-(4-methylpyridine) thiocyanates and related
342 compounds. *J. Chem. Soc.A* **1969**, 1717-1723.
- 343 7. Barrer, R.M.; Galabova, I.M. Ion-Exchanged Forms of Zeolite L, Erionite, and Offretite and Sorption of Inert Gases. *Adv. Chem.*
344 *Ser.* **1973**, *121*, 1-28.
- 345 8. Grafkskaia, K.N.; Anokhin, D.V.; Zimka, B.I.; Izdelieva, I.A.; Zhu, X.; Ivanov, D.A. An “on-off” switchable cubic phase with
346 exceptional thermal stability and water sorption capacity. *Chem. Commun.* **2017**, *53*, 13217-13220.
- 347 9. Sirringhaus, H.; Brown, P.J.; Friend, R. H.; Nielsen, M. M.; Bechgaard, K.; Langeveld-Voss, B. M. W.; Spiering, A. J. H.; Janssen,
348 R. A. J.; Meijer, E. W.; Herwig, P.; de Leeuw, D. M. Two-dimensional charge transport in self-organized, high-mobility conju-
349 gated polymers. *Nature* **1999**, *401*, 685-688.

- 350 10. Hosono, N.; Kajitani, T.; Fukushima, T.; Ito, K.; Sasaki, S.; Takata, M.; Aida, T. Large-Area Three-Dimensional Molecular Or-
351 dering of a Polymer Brush by One-Step Processing. *Science* **2010**, *330*, 808-811.
- 352 11. Grelet, E.; Bock, H. Control of the orientation of thin open supported columnar liquid crystal films by the kinetics of growth.
353 *Europhys. Lett.* **2006**, *73*, 712-718.
- 354 12. Majewski, P.W.; Gopinadhan, M.; Jang, W.S.; Lutkenhaus, J.L.; Osuji, C.O. Anisotropic Ionic Conductivity in Block Copolymer
355 Membranes by Magnetic Field Alignment. *J. Am. Chem. Soc.* **2010**, *132*(49), 17516-17522.
- 356 13. Tousley, M.E.; Feng, X.; Elimelech, M.; Osuji, C.O. Aligned Nanostructured Polymers by Magnetic-Field-Directed
357 Self-Assembly of a Polymerizable Lyotropic Mesophase. *ACS Appl. Mater. Interfaces* **2014**, *6*(22), 19710-19717.
- 358 14. Vita, F.; Hegde, M.; Portale, G.; Bras, W.; Ferrero, C.; Samulski, E.T.; Francescangeli, O.; Dingemans, T. Molecular ordering in
359 the high-temperature nematic phase of an all-aromatic liquid crystal. *Soft Matter* **2016**, *12*, 2309-2314.
- 360 15. Feng, X.; Tousley, M. E.; Cowan, M. G.; Wiesenauer, B. R.; Nejadi, S.; Choo, Y.; Noble, R.D.; Elimelech, M.; Gin, D. L.; Osuji, C.
361 O. Scalable Fabrication of Polymer Membranes with Vertically Aligned 1 nm Pores by Magnetic Field Directed Self-Assembly.
362 *ACS Nano* **2014**, *8*(12), 11977-11986.
- 363 16. Zhu, X.; Tartsch, B.; Beginn, U.; Möller, M. Wedge-Shaped Molecules with a Sulfonate Group at the Tip—A New Class of
364 Self-Assembling Amphiphiles. *Chem. Eur. J.* **2014**, *10*, 11977-11986.
- 365 17. Pifferi, G.; Monguzzi, R. New compounds: Synthesis of 3,4,5-trimethoxybenzenesulfonamides. *J. Pharm. Sci.* **1973**, *63*,
366 1392-1394.
- 367 18. Zhu, X.; Beginn, U.; Möller, M.; Gearba, R.I.; Anokhin, D.V.; Ivanov, D.A. Self-Organization of Polybases Neutralized with
368 Mesogenic Wedge-Shaped Sulfonic Acid Molecules: An Approach toward Supramolecular Cylinders. *J. Am. Chem. Soc.* **2006**,
369 *128*, 16928-16937.
- 370 19. Zhu, X.; Scherbina, M.A.; Bakirov, A.V.; Gorzolnik, B.; Chvalun, S.N.; Beginn, U.; Moeller, M. Methacrylated Self-Organizing
371 2,3,4-Tris(alkoxy)benzenesulfonate: A New Concept Toward Ion-Selective Membranes. *Chem. Mater.* **2006**, *18*, 4667-4673.
- 372 20. Beginn, U.; Yan, L.; Chvalun, S.N.; Shcherbina, M.A.; Bakirov, A.; Moeller, M. Thermotropic columnar mesophases of
373 wedge-shaped benzenesulfonic acid mesogens. *Liquid Crystals* **2008**, *35*(9), 1073-1093.
- 374 21. Shcherbina, M.A.; Bakirov, A.V.; Yakunin, A.N.; Beginn, U.; Yan, L.; Moeller, M.; Chvalun, S.N. The effect of the shape of the
375 mesogenic group on the structure and phase behavior of 2,3,4-tris(dodecyloxy)benzenesulfonates with alkaline cations. *Soft*
376 *Matter* **2014**, *10*, 1746-1757.
- 377 22. Shcherbina, M.A.; Bakirov, A.V.; Yan, L.; Beginn, U.; Zhu, X.; Moeller, M.; Chvalun, S.N. Heuristics for precise supramolecular
378 control of soft matter structure and properties – 2,3,4-tris(dodecyloxy)benzenesulfonates with alkaline and organic cations.
379 *Mendeleev Commun.* **2015**, *5*, 142-144.
- 380 23. Garstecki, P., Holyst, R. Scattering Patterns of Multiply Continuous Cubic Phases in Block Copolymers. I. The Model. *Macro-*
381 *molecules* **2003**, *36*, 9181-9190.
- 382